UDC 532.6:517.9 **doi: 10.32620/reks.2025.1.08**

Vitalii MYNTIUK[1], Olga SHYPUL[1], Oleh TRYFONOV[1], Yevgen TSEGELNYK[2]

[1] ***National Aerospace University "Kharkiv Aviation Institute", Kharkiv, Ukraine***
[2] ***O. M. Beketov National University of Urban Economy in Kharkiv, Kharkiv, Ukraine***

AXISYMMETRIC PROBLEM OF SMOOTHING THE SURFACE OF A VISCOUS LIQUID BY SURFACE TENSION FORCES

*This study investigates **an analytical solution to the problem of the surface levelling of viscous liquids under the influence of surface tension forces**, focusing on the smoothing of plastic surfaces subjected to thermal energy treatment. This study **aims** to extend Orchard's formula to axisymmetric surface irregularities and develop an analytical model for predicting levelling time, thereby ensuring efficient process control in thermal treatment applications. The **tasks** included deriving an analytical solution for axisymmetric levelling, validating it against numerical simulations in LS-DYNA, and incorporating the viscosity variation across the liquid layer. The **methods** involved analytical formulation and numerical simulation of surface evolution considering different initial surface geometries and viscosity distributions. Validation against numerical results demonstrated high accuracy for moderate and thick liquid layers ($h > 0.2R$) and initial surface amplitudes up to 40% of the characteristic radius. Following validation, the model was applied to estimate levelling times for various surface configurations while maintaining simplicity while improving the predictive capabilities. **Results** showed that the extended formula effectively describes surface smoothing dynamics, including the cases with thickness-dependent viscosity, providing explicit expressions for levelling time. These findings enable precise control of heat input during thermal energy treatment, thereby optimizing the surface quality. In **conclusion**, the proposed analytical solutions offer a practical tool for surface levelling analysis, expanding the applicability of Orchard's approach to more complex geometries and viscosity variations. In future work, we will focus on experimental validation and refinements to enhance the accuracy in industrial applications.*

Keywords: *Surface Levelling; Orchard's Formula; Axisymmetric Irregularities; Periodic Problem Formulation.*

1. Introduction

1.1. Motivation

The finishing of thermoplastic parts is critical for meeting the high demands for accuracy and quality in industries such as automotive, aerospace, and healthcare. Engineering and high-performance plastics are valued for their low weight, high strength, and corrosion resistance, making them ideal for applications in which precision and durability are paramount [1]. However, manufacturing processes like injection molding and additive manufacturing often result in surface defects such as burrs, flashes, and roughness, which can compromise reliability, lifetime, and functional characteristics [2].

Additive manufacturing, particularly Fused Deposition Modeling (FDM), has seen widespread adoption [3]. FDM parts, however, frequently exhibit poor surface finish due to visible layer lines and micropores, as illustrated in studies showing nylon samples with line-by-line filament separation and polylactic acid parts with surface micropores [4]. These defects not only affect aesthetics but also mechanical properties, necessitating advanced finishing techniques.

Traditional surface finishing methods include mechanical abrasion, chemical treatment, ultrasonic vibration processing, and blasting. However, these methods have significant limitations, especially for complex geometries and when high surface smoothness is required. For instance, abrasive methods may alter part dimensions, whereas chemical treatments may not be suitable for all materials and situations [5]. Thermal methods, such as hot air jet polishing and laser-based thermal polishing, have been explored; however, they can be time-consuming or inefficient for deep holes and complex shapes [6, 7].

The Impulse Thermal Energy Method (ITEM), a variation of the Thermal Energy Method (TEM), offers a promising solution by leveraging controlled heat exposure to melt the surface layer, allowing surface tension to smooth out irregularities. ITEM operates in a closed chamber, using combustion products to provide precise heat input, which is crucial for thermoplastics to avoid carbonization and soot deposition [8]. Unlike standard TEM, which uses oxygen-excess mixtures suitable for metal parts, ITEM employs stoichiometric or fuel-rich mixtures, ensuring the safety and integrity of thermoplastic surfaces.

The motivation for this study lies in the development of an analytical model to predict the levelling time during ITEM processing, focusing on axisymmetric surface irregularities. This is particularly relevant for post-additive manufacturing parts, where the surface quality directly affects the overall performance. An analytical solution would facilitate process control, optimize heat input, and enhance efficiency, addressing the gap in current methods that often rely on empirical adjustments or numerical simulations, which can be time-consuming and less intuitive for industrial applications.

1.2. State of the Art

Orchard's formula, which was first introduced in 1963, provides a foundational analytical solution for the surface levelling of viscous liquids, which was initially applied to paint films with periodic stripe-like irregularities [9]. The formula relates the levelling time to the surface tension, viscosity, and initial amplitude of the surface perturbations, offering a balance between simplicity and practical utility. The validity of the proposed method has been experimentally confirmed by researchers such as Wapler [10] and Overdiep [11], with extensions to include surface tension gradients for viscosity changes during solvent evaporation. Extensions of Orchard's formula have been proposed to address more complex scenarios. For instance, Weidner [12] considered two-component fluids with yield stress, leading to distinct flow regimes that required numerical solutions using finite difference methods. Seeler et al. [13] developed numerical approaches for thixotropic paints, using Orchard's solution as a benchmark for idealized sinusoidal films. These refinements, while enhancing accuracy, often sacrifice the analytical simplicity that makes Orchard's formula valuable for industrial applications, such as viscosity determination from sinusoidal film amplitude measurements [14] and modelling levelling times in roll-coating processes [15]. In paper [16], a theoretical tool was proposed as an alternative perspective on surfactant forces at interface boundaries, allowing the known equations to be rewritten by calculating the balance of forces in the steady state. Furthermore, Takahashi *et al.* [17] used this formula to study the time-dependent variation of viscosity. In a broader context, heat transfer studies involving multilayer shells with non-stationary temperature fields have demonstrated the importance of accurately modelling the thermal effects in coated and layered materials [18]. Similarly, transient thermoelastic analysis of cylindrical structures with varying coefficients of thermal expansion has been explored to determine the effects of heat flux on the stress distribution [19].

In the context of thermoplastic parts, various finishing methods have been employed, as detailed by Plankovskyy *et al.* [8]. Mechanical methods like CNC machining and barrel treatment are common; however, they may not be sufficient for complex geometries [20]. Chemical methods show promise for reducing roughness, but they are material-specific [21]. Thermal methods, such as hot air jet polishing, use surface tension in the melted layer, but are time-consuming for intricate shapes [6]. Laser-based thermal polishing, as explored by Chai *et al.* [7], considers surface over-melt (SOM) and surface shallow-melt (SSM) mechanisms, with SOM potentially removing micropores but varying in efficacy across materials.

The ITEM stands out for its controlled heat exposure, which uses combustion products in a closed chamber to prevent damage to thermoplastics. Unlike TEM, which is optimized for metal parts with oxygen-excess mixtures, ITEM uses stoichiometric or fuel-rich mixtures to avoid carbonization, a critical consideration given the potential for toxic gas formation in thermoplastics like polyvinyl chloride [8]. The selection of ITEM processing regimes involves the design of the experimental method, which can be time-consuming, especially for complex shapes, highlighting the need for automated approaches based on numerical simulation [22].

Despite these advancements, there is a notable gap in analytical models for predicting levelling time in axisymmetric geometries, particularly for thermoplastic parts post-additive manufacturing. Current research lacks a simple, generalizable solution that can be readily applied in industrial settings, where process control and efficiency are paramount. This study aims to bridge this gap by extending Orchard's formula and leveraging the principles of surface tension and viscosity to model surface evolution in three-dimensional, radially symmetric configurations.

1.3. Objective and Approach

This study extends Orchard's formula to axisymmetric surface irregularities and addresses its applicability to surface smoothing during ITEM processing of thermoplastic parts. The primary objective is to develop a simple yet effective analytical model for predicting surface levelling time, thereby ensuring precise control of heat input in industrial applications. The proposed approach involves the following steps:

– deriving an analytical solution for surface levelling with axisymmetric irregularities;

– validating the solution against numerical simulations performed using LS-DYNA;

– extending the model to account for viscosity variations across the liquid layer thickness.

The proposed analytical solutions maintain the simplicity of Orchard's original formulation while expanding its applicability to complex levelling scenarios. By explicitly determining the surface smoothing time, the developed model provides a practical tool for optimizing ITEM processing, thereby enabling efficient material treatment and improved surface quality.

This paper is organized as follows. Section 2 defines the problem statement, focusing on surface levelling in thermal energy treatment. Section 3 develops the mathematical model and extends Orchard's formula. The analytical solution is presented in Section 4. In Section 5, the model is validated against LS-DYNA simulations. Section 6 examines the effects of variable viscosity. Section 7 generalizes the proposed approach to arbitrary surface shapes. Section 8 discusses the implications of the study findings. Section 9 concludes with a summary of the key findings.

2. Problem Statement

The problem statement and essentially the solution coincide with those given in [9] except for the domain in which the problem is solved. While in the paper of Orchard an infinite strip with a periodic waveform (a plane problem) was considered (Fig. 1,*a*), in this study an axisymmetric problem was considered (Fig. 1,*b*).

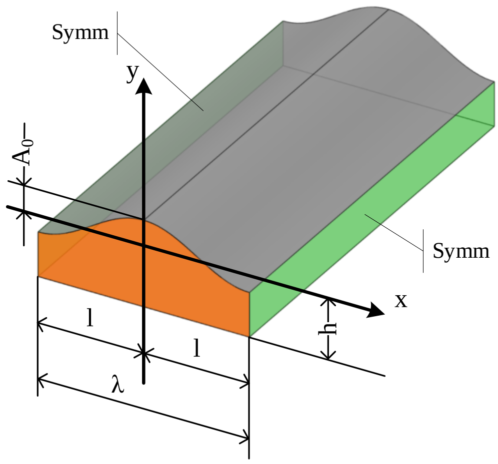

(*a*)

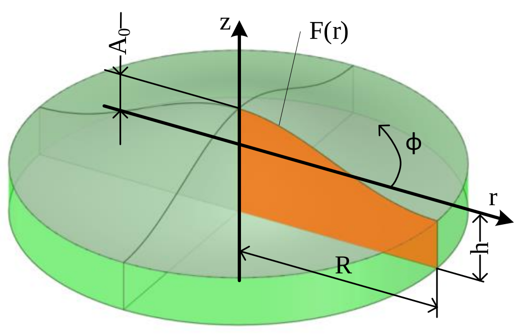

(*b*)

Fig. 1. Schematic representation of the film: (*a*) is the periodic Orchard problem; (*b*) is the axisymmetric problem this study

Absolute dimensions are considered to be approximately 1 mm or less, allowing us to neglect the forces of gravity. Thus, if the maximum hydrostatic pressure at the wave height (Fig. 1,*a*) is equal to $p_g = 2\rho g A_0$, and the maximum pressure from surface tension forces according to the Laplace equation is $p_\gamma = \gamma k = \gamma \frac{\pi^2 A_0}{l^2}$, then the ratio of these pressures is $\frac{p_g}{p_\gamma} = \frac{2\rho g}{\pi^2 \gamma} l^2$, i.e. for liquids with a significant surface tension force ($\gamma > 20$ mN/m), a density less than, or of the same order as water ($\approx$ 1000 kg/m^3) and a half-wavelength of 1 mm, the hydrostatic pressure will be less than 10% of the surface tension pressure, with a half-wavelength of 0.5 mm, it will be less than 3%.

Velocities and accelerations are also considered small, which allows us to neglect inertial forces and, accordingly, oscillatory processes. The fluid has Newtonian properties.

3. Mathematical model

The Navier-Stokes equation and the continuity equation in the polar coordinate system (Fig. 1,*b*), considering the assumptions made, take the form of

$$\mu\left[\frac{\partial u}{\partial r}\left(\frac{1}{r}\frac{\partial}{\partial r}(ru)\right) + \frac{\partial^2 u}{\partial z^2}\right] = \frac{\partial p}{\partial r},$$
$$\mu\left[\frac{1}{r}\frac{\partial w}{\partial r}\left(r\frac{\partial w}{\partial r}\right) + \frac{\partial^2 w}{\partial z^2}\right] = \frac{\partial p}{\partial z}, \tag{1}$$

$$\frac{1}{r}\frac{\partial}{\partial r}(ru) + \frac{\partial w}{\partial z} = 0, \tag{2}$$

where u, w are the velocities in the radial and vertical directions, respectively; p is the pressure; μ is the dynamic viscosity.

Boundary conditions. At the bottom edge $z = -h$, no slip conditions are imposed:

$$u = w = 0. \tag{3}$$

We assume that the upper edge $z = F(r)$, where $F(r)$ is the equation of the free surface, deviates little from the level $z = 0$, therefore, we require the fulfillment of the conditions on this edge at $z = 0$. On this edge, assuming the small of the deviation of the free surface, we have:

- condition of absence of tangential stresses

$$\tau_{rz} = \mu\left(\frac{\partial u}{\partial z} + \frac{\partial w}{\partial r}\right) = 0; \tag{4}$$

- equilibrium between normal stresses and external pressure (pressure from surface tension forces)

$$\sigma_z = -p + 2\mu\frac{\partial w}{\partial z} = p_{st}. \tag{5}$$

The pressure due to surface tension forces is determined by Laplace's equation

$$p_{st} = \gamma\left(\frac{1}{R_1} + \frac{1}{R_2}\right), \tag{6}$$

where γ is the surface tension; $\frac{1}{R_1}$ and $\frac{1}{R_2}$ are the principal curvatures of the free surface, which, considering axial symmetry, are determined through the function that defines the free surface $F(r)$

$$\frac{1}{R_1} = \frac{d^2F}{dr^2}\left[1 + \left(\frac{dF}{dr}\right)^2\right]^{-\frac{3}{2}}, \tag{7}$$

$$\frac{1}{R_2} = \frac{1}{r}\frac{dF}{dr}\left[1 + \left(\frac{dF}{dr}\right)^2\right]^{-\frac{1}{2}}. \tag{8}$$

Symmetry conditions are imposed on the edge $r = R$:

$$u = \frac{\partial w}{\partial r} = \frac{\partial p}{\partial r} = 0. \tag{9}$$

Thus, the mathematical model of the problem is formulated using three differential equations (1), (2) in the region occupied by the liquid and a set of boundary conditions (3)–(5), (9).

4. Problem Solution

In such a formulation, the problem allows for the separation of variables in the domain, and boundary conditions (9) can be automatically satisfied if a solution is sought in the form

$$\begin{aligned} u(r,z) &= \textstyle\sum_{n=1,2,...} U(z) J_1(\lambda_n r) \\ w(r,z) &= \textstyle\sum_{n=1,2,...} W(z) J_0(\lambda_n r), \\ p(r,z) &= \textstyle\sum_{n=1,2,...} P(z) J_0(\lambda_n r) \end{aligned} \tag{10}$$

where J_0, J_1 are the Bessel functions of the first kind of zero and first order; $\lambda_n = \frac{b_n}{R}$, b_n is the zeros of the function, $,J_1; b_1 = 3.8317060$, $b_2 = 7.0155867$, $b_3 = 10.173468$, ...; $U(z), V(z), P(z)$ are the functions that are still unknown.

If we substitute the solutions (10) into the differential equations (1), (2), then, given the linear independence of the functions J_0, J_1, we obtain a systems of ordinary differential equations with respect to the functions $U(z), W(z), P(z)$:

$$\begin{cases} \frac{d^2U(z)}{dz^2} - \lambda_n^2 U(z) + \frac{\lambda_n}{\mu} P(z) = 0, \\ \frac{d^2W(z)}{dz^2} - \lambda_n^2 W(z) - \frac{1}{\mu}\frac{dP(z)}{dz} = 0, \\ \lambda_n U(z) + \frac{dW(z)}{dz} = 0, \end{cases} \tag{11}$$

where $n = 1,2,3, ...$

Integrating the n^{th} system of equations (11) leads to the following solutions

$$\begin{aligned} U(z) &= \left(c_4 z + c_2 - \frac{c_3}{\lambda}\right)\cosh(\lambda z) - \\ &- \left(c_3 z + c_1 - \frac{c_4}{\lambda}\right)\sinh(\lambda z), \\ W(z) &= (c_3 z + c_1)\cosh(\lambda z) - \\ &-(c_4 z + c_2)\sinh(\lambda z), \\ P(z) &= 2\mu\big(c_3\cosh(\lambda z) - c_4\sinh(\lambda z)\big), \end{aligned} \tag{12}$$

here and below, to reduce the notation for $\lambda, U(z), V(z), P(z)$ and the constants of integration c_i, the index ‘n’ is omitted.

The four integration constants $c_i$are found from the boundary conditions (3)–(5). To implement condition (5) when determining the pressure from surface tension forces (6) the function of the free surface is given in the form of a Fourier series on the segment $-R \le r \le R$ in terms of the functions J_0:

$$F(r) = \textstyle\sum_{n=1,2,...} A_n J_0(\lambda_n r). \tag{13}$$

Note that this function has a property $\int_{-R}^{R} rF(r)\,dr = 0$ that physically means the equality of the volumes of the liquid above the coordinate plane $r\varphi$ and the cavity below it (Fig. 1,*b*).

If we consider the function $F(r)$ to be flat (surface gradient is small), $\frac{dF}{dr} \ll 1$ i.e., when determining the curvatures (7) we neglect the expressions in square brackets, then, again omitting the index ‘n’, we obtain the expression of the n^{th} pressure component, from the surface tension forces (6) in the form of

$$p_{st} = -\gamma A\lambda^2 J_0(\lambda r). \tag{14}$$

Thus, equations (3)–(5) for determining the integration constants c_i considering the expressions for the desired functions (10) and (12) take the form of

$$\begin{gathered} \left(c_2 - c_4 h - \frac{c_3}{\lambda}\right)\cosh(\lambda h) + \\ + \left(c_1 - c_3 h - \frac{c_4}{\lambda}\right)\sinh(\lambda h) = 0, \\ (c_1 - c_3 h)\cosh(\lambda h) + (c_2 - c_4 h)\sinh(\lambda h) = 0, \\ c_4 - c_1\lambda = 0, \\ 2\mu c_2 = \gamma A\lambda. \end{gathered}$$

The solution of these equations leads to the same expressions for the coefficients c_i as in [9] with the exception that here $\lambda_n = \frac{b_n}{R}$ instead of the analogous quantity in Orchard's solution $k_n = \frac{n\pi}{l}$

$$c_1 = -\frac{\gamma A \lambda}{2\mu} f(\theta),\ c_2 = \frac{\gamma A \lambda}{2\mu},$$
$$c_3 = \frac{\gamma A \lambda^2}{2\mu} g(\theta),\ c_4 = -\frac{\gamma A \lambda^2}{2\mu} f(\theta), \quad (15)$$

here, also following [1], the notation is shortened for brevity:

$$\theta = \lambda h,$$
$$f(\theta) = \frac{\sinh(2\theta) - 2\theta}{1 + 2\theta^2 + \cosh(2\theta)}, \quad (16)$$
$$g(\theta) = \frac{1 + \cosh(2\theta)}{1 + 2\theta^2 + \cosh(2\theta)}.$$

Finally, the solutions (10) can be determined by the geometric parameters, viscosity, and surface tension coefficient.

The rate of amplitude A change is determined from the condition of equality between the found velocity $w(r, 0)$ and the velocity of the upper limit $\frac{\partial F}{\partial t}$

$$\sum_{n=1,2,\ldots} -\frac{\gamma A_n \lambda_n}{2\mu} f(\theta) J_0(\lambda_n r) =$$
$$= \sum_{n=1,2,\ldots} \frac{\partial A_n}{\partial t} J_0(\lambda_n r),$$

which leads to systems of differential equations as follows:

$$\frac{\partial A}{\partial t} + A \frac{\gamma \lambda}{2\mu} f(\theta) = 0, \quad (17)$$

the integral of which, considering the initial condition $A(t = 0) = A_0$, has the following form

$$A(t) = A_0 \exp\left(-\frac{\gamma \lambda t}{2\mu} f(\theta)\right). \quad (18)$$

Formula (18) is the main practical result, as it clearly shows that the amplitude of the convexity (unevenness) and the speed decrease exponentially in time. The dependence on the convexity geometry is hidden in the function $f(\theta)$. Recall that the dimensionless parameter approximations $\theta = \lambda h = b_n \frac{h}{R}$ is essentially a relative average thickness. The function $f(\theta)$ has asymptotic approximation [9]: at $\theta \to 0$, $f(\theta) \to \frac{2}{3}\theta^3$ and $\theta \to \infty$, $f(\theta) \to 1$. Fig. 2. shows the graphs of the function in the logarithmic coordinate system and the usual coordinate system. The vertical lines mark the limits at which the approximation errors exceeded. That is, the form of the function $f(\theta) = \frac{2}{3}\theta^3$ can be taken at $\theta < 0.167$ $(h < 0.217R)$, and $f(\theta) = 1$ at $\theta > 3.62$ $(h > 4.72R)$, at the same time the error caused by such a replacement will not exceed 5%.

As noted above, the difference between solution (18) and solution [9] consists in calculating the parameter λ, if in the solution (18) the calculation uses the first root of the Bessel function of the first kind $(b_1 = 3.8317060)$ is used in the calculation, then the solution [9] is $\pi = 3.1415927$. The quantitative differences in the solutions with respect to the relative average thickness are shown in Fig. 3. When calculating the values of the functions, a dimensionless time $T = \frac{\gamma t}{\mu R} = \frac{\gamma t}{\mu l}$ was introduced.

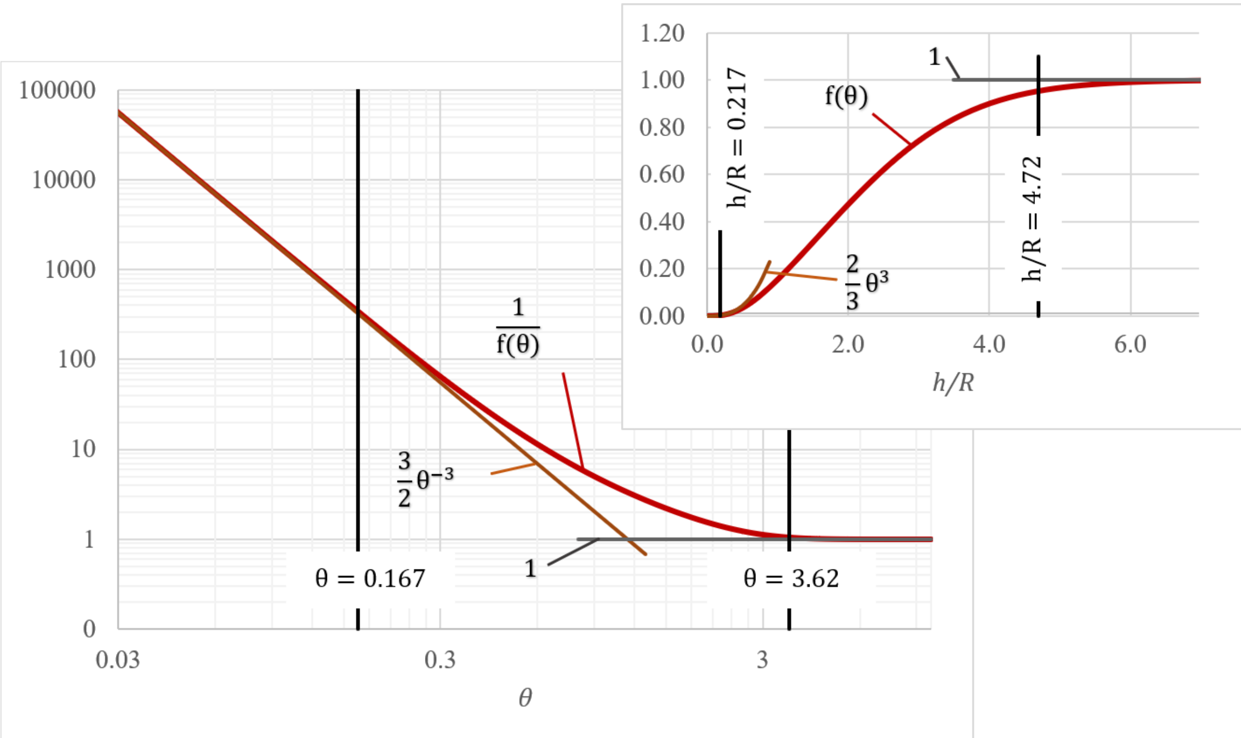

Fig. 2. Asymptotic approximation of the function $f(\theta)$

ISSN 1814-4225 (print)
ISSN 2663-2012 (online)

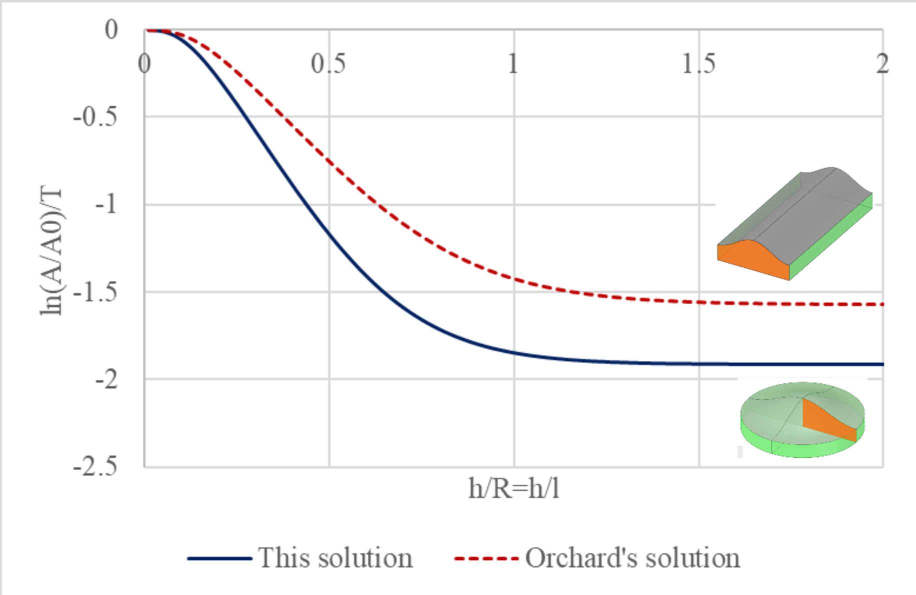

Fig. 3. Comparison of periodic and asymptotic solutions

As can be seen, the rate of decrease in the amplitude in both cases has the same character, but in the axisymmetric case the rate is higher, which is explained by the presence of additional curvature in the circumferential direction (6), which leads to an increase in the pressure from the surface tension.

5. Comparison with Numerical Simulation Results

The numerical solution of the problem was obtained using the Incompressible Smoothed Particle Galerkin (ISPG) method, which was implemented in the LS-DYNA software. The proposed method is a modified SPG method in which the formulation is based on a smoothed displacement field in a meshless Galerkin variational structure. The method is modified for modelling Newtonian and non-Newtonian fluids with free surfaces, considering surface tension and adhesion forces. The discretization of the Navier-Stokes equations in the ISPG method is implemented based on the Lagrangian approach, which provides an accurate integration of the interactions of fluids with rigid structures. The ISPG method and its theory are described in detail in [23]. Another approach is presented in [24], where the particle-scale surface tension force (STF) model is incorporated into the smoothed particle hydrodynamics (SPH) method.

The computational model of the test problem is shown in Fig. 4. One quarter of the volumetric region is considered. Size $R = 5$ mm. Characteristics of a liquid (such as cooking oil) $\mu = 0.2\ \mathrm{Pa \cdot s}, \gamma = 0.02\ \frac{\mathrm{N}}{\mathrm{m}}$. The conditions of interaction between a liquid and a solid on a cylindrical vertical surface are given as free sleep with a free surface contact angle of 90°. No slip conditions were set on the lower horizontal surface.

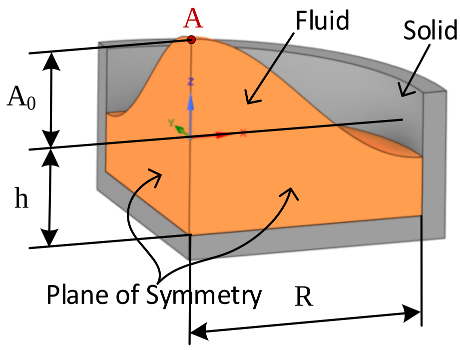

Fig. 4. Calculation model

To completely exclude inertial forces from the calculation, an almost zero density of the material was set $1\ \frac{\mathrm{kg}}{\mathrm{m}^3}$. The average thickness $h =$ 0.3; 0.6; 1.0; 2.0; 3.0; 6.0 mm and the initial amplitude $A_0 = 0.5$; 1.0; 2.0; 3.0; 4.0 mm were varied in the calculations.

A qualitative comparison of the velocities and pressures distribution were obtained analytically and numerically are shown in Fig. 5, using the example of $A_0 = 0.5$ mm, $h = 2$ mm at the initial time. The horizontal (radial) velocity has a peak at the center and a slight shift toward the free surface. The maximum vertical velocities are realized at the edge and in the centre of the free surface, where the velocity in the centre is approximately three times higher than the velocity at the edge.

There is a similar noticeable difference in the pressure values; however, unlike the vertical velocity, the pressure decay into depth is almost absent. In general, it can be noted that the analytical and numerical solutions agreed well. The changes in amplitude over time (position of point A, Fig. 4) were quantitatively compared and thoroughly investigated.

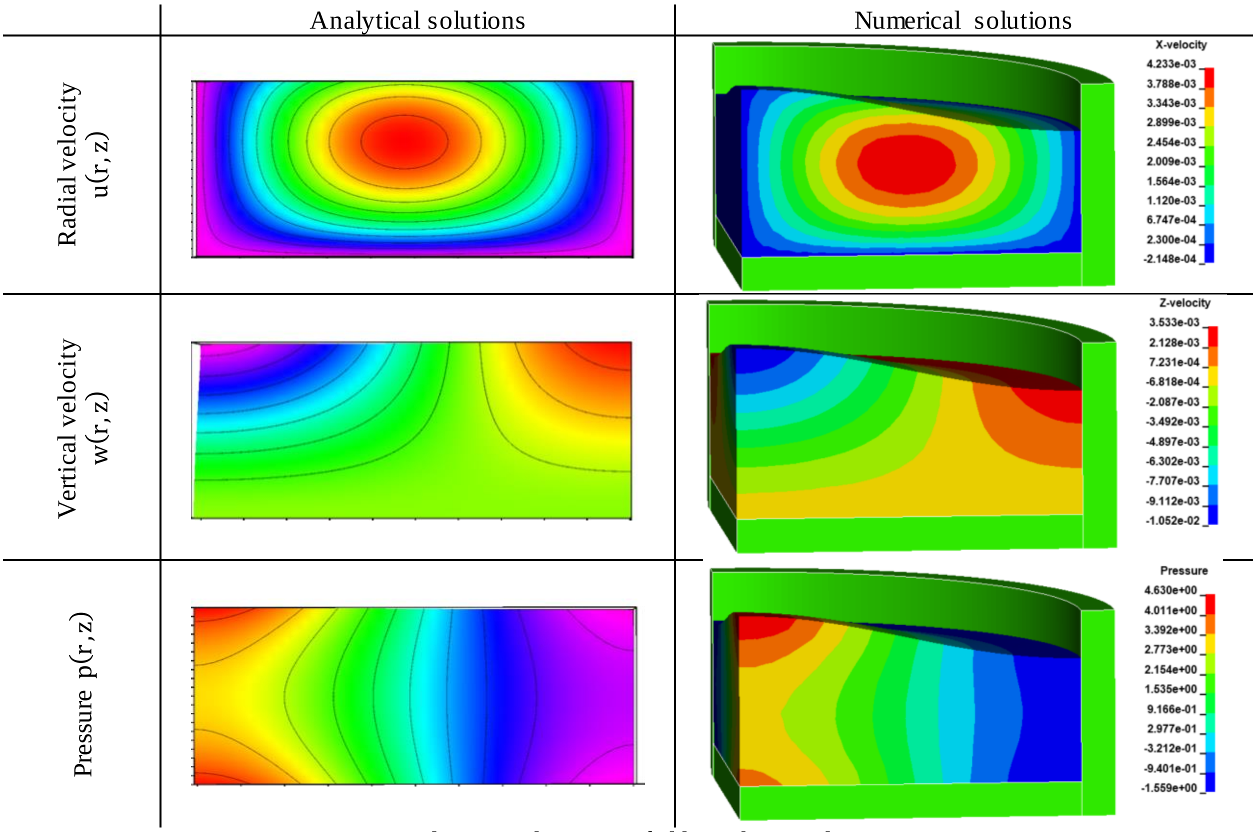

Fig. 5. Velocity and pressure fields at the initial moment
(color scales for analytical and numerical solutions are different)

The study aimed to identify the error in the analytical solution, which is introduced when satisfying the boundary conditions on the upper boundary:

– fulfilling the boundary conditions (4), (5) on the edge $z = 0$, and not $z = F$;

– using the stresses τ_{rz} and σ_z in the conditions (4), (5), and not to the returned tangent and normal stresses $\tau_\alpha = \frac{\tau_{rz}(1-(F')^2)+(\sigma_r-\sigma_z)F'}{(F')^2+1}$ and $\sigma_\alpha = \frac{\sigma_z+(F')^2\sigma_r+2F'\tau_{rz}}{(F')^2+1}$;

– neglecting the denominators when calculating the curvatures (7).

In the numerical solution, these assumptions are, of course, not accepted, while the remaining assumptions used in building the model are the same in both cases.

The relative changes in amplitudes (A/A_0) in dimensionless time $\left(\bar{t} = \frac{\gamma\lambda t}{2\mu}\right)$, obtained numerically for various combinations of relative average thickness (h/R) and relative initial amplitude (A_0/R), are shown in Fig. 6. It can be seen that slight deviations from linear behavior are observed for configurations with a large initial amplitude. The influence of the relative initial amplitude on the smoothing rate (in the analytical solution such influence is absent) increases with increasing average thickness.

To quantitatively compare analytical solutions with numerical solutions, the curves shown in Fig. 6 were linearized by the least squares method, i.e., they were reduced to the form $A = A_0 \exp(-C\bar{t})$, where $\bar{t} = \frac{\gamma\lambda}{2\mu} t$ is dimensionless time. The values of the coefficients C determined in this way are shown in Table 1 and Fig. 7.

As can be seen, the assumption of the smoothness of the free surface of the liquid is valid in a fairly wide range, so for moderate and thick films the analytical solution can be considered reliable at a relative initial amplitude of up to 40% (the error does not exceed 10%). However, for thin films, there is a significant discrepancy between the analytical and numerical solutions. The numerical solution shows a considerably higher surface smoothing rate, and this is not related to the smoothness of the free surface.

6. Variable Viscosity

If we consider the heat treatment of plastic surfaces, that is, the heating and melting of the surface layer to a certain depth, then the temperature will spread unevenly into the depth, to be more precise, this dependence when heated by a heat flow has the following form

$$T = Q\left[2\sqrt{\frac{\alpha t}{\pi}}\, e^{-\frac{z^2}{4\alpha t}} - z\,\mathrm{erfc}\left(\frac{z}{2\sqrt{\alpha t}}\right)\right],$$

where Q is the heat flux; α is the thermal diffusivity; erfc is the complementary error function.

ISSN 1814-4225 (print)
ISSN 2663-2012 (online)

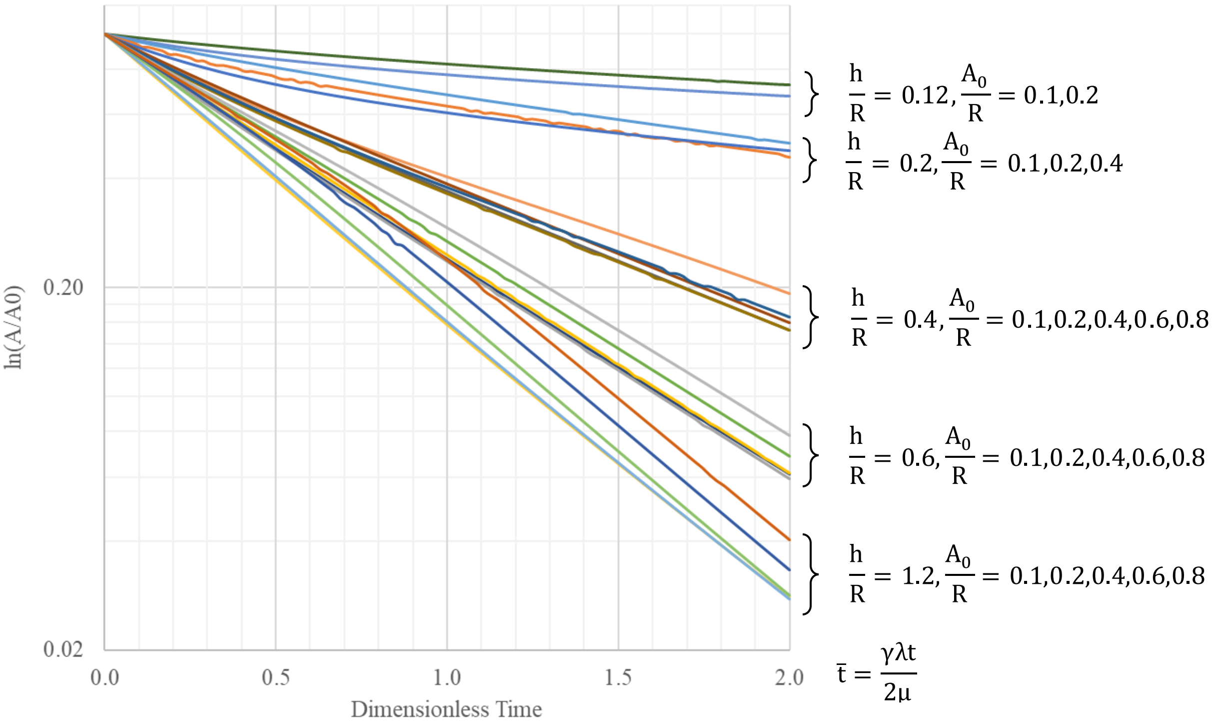

Fig. 6. Relative changes in amplitudes over dimensionless time

Table 1

Coefficient C values when determining amplitude $A = A_0 \exp(-C\bar{t}) = \exp\left(-C\frac{\gamma\lambda}{2\mu}t\right)$

h, mm	h/R	kh	Amplitude, mm					Analytical
			0.5	1	2	3	4	
			A/R					
			0.1	0.2	0.4	0.6	0.8	
0.3	0.06	0.2299	 0.0440					0.0074
0.6	0.12	0.4598	 0.0940	 0.1258				0.0470
1	0.2	0.7663	 0.1943	 0.2282	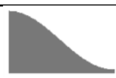 0.2415			0.1467
2	0.4	1.5327	 0.4913	 0.5120	 0.5180	 0.4974	 0.4601	0.4642
3	0.6	2.2990	 0.7413	 0.7489	 0.7316	 0.6925	 0.6527	0.7357
6	1.2	4.5980	 0.9529	 0.9460	 0.9093	 0.8464	 0.7857	0.9894

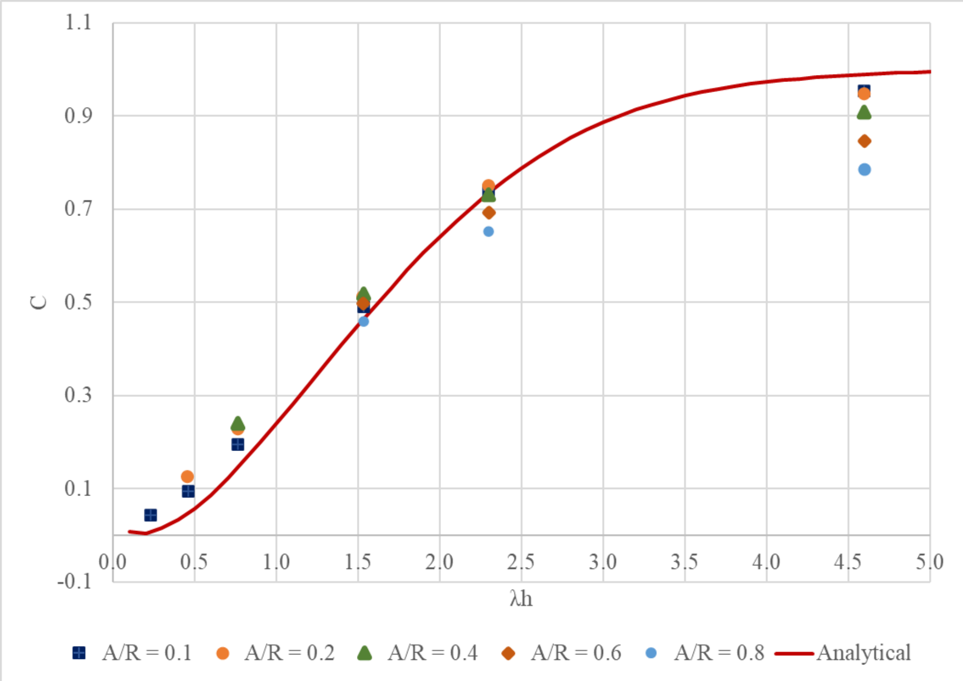

Fig. 7. Coefficient C value when determining amplitude $A = A_0 \exp(-C\bar{t}) = \exp\left(-C\frac{\gamma\lambda}{2\mu}t\right)$

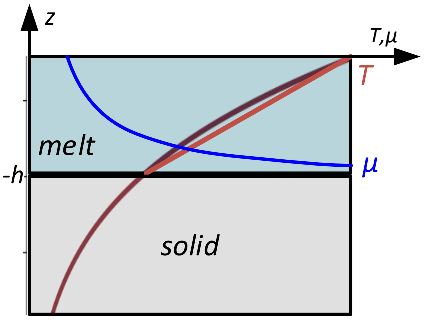

Fig. 8. Temperature distribution in depth and viscosity changes

Approximately in the surface molten layer (Fig. 8) the temperature distribution can be assumed to be linear and, if we assume that the fluidity is directly proportional to the temperature, then in the first approximation we can assume its linear change – from the maximum value on the surface to zero at the melting point. The viscosity in this case changes from a finite value μ on the surface to infinity when approaching the solid phase (Fig. 8). In this case, unlike in Section 3, the differential equations (1) takes the following form

$$\mu\frac{h}{h+z}\left[\frac{\partial u}{\partial r}\left(\frac{1}{r}\frac{\partial}{\partial r}(ru)\right)+\frac{\partial^2 u}{\partial z^2}\right]=\frac{\partial p}{\partial r},$$
$$\mu\frac{h}{h+z}\left[\frac{1}{r}\frac{\partial w}{\partial r}\left(r\frac{\partial w}{\partial r}\right)+\frac{\partial^2 w}{\partial z^2}\right]=\frac{\partial p}{\partial z}. \qquad (19)$$

The remaining ratios are unchanged. The solution is constructed similarly to that done in section 4. Functions (12) after the separation of variables and the solution of the system of ordinary differential equations take the following form

$$U(z) = -d_1\sinh(\lambda z) - d_2\cosh(\lambda z) -$$
$$-(h+z)^2\left[d_3 I_1\big(\lambda(h+z)\big) - d_4 K_1\big(\lambda(h+z)\big)\right],$$
$$W(z) = d_1\cosh(\lambda z) + d_2\sinh(\lambda z) +$$
$$+(h+z)^2\left[d_3 I_0\big(\lambda(h+z)\big) + d_4 K_0\big(\lambda(h+z)\big)\right] -$$
$$-\frac{2}{k}(h+z)\left[d_3 I_1\big(\lambda(h+z)\big) - d_4 K_1\big(\lambda(h+z)\big)\right],$$
$$P(z) = 3\mu h\left[d_3 I_0\big(\lambda(h+z)\big) + d_4 K_0\big(\lambda(h+z)\big)\right], \qquad (20)$$

where $I_0, I_1, K_{,0} K_1$ are modified Bessel functions of the first and second kinds, zero and first order.

The integration constants d_i are determined from the boundary conditions (3)–(5)

$$d_{1/2} = \frac{2}{\Delta}\left(e^{2\theta} \pm 1\right)\left(2\theta I_0(\theta) - I_1(\theta)\right),$$
$$d_3 = \frac{2}{\Delta}\left[\theta e^{\theta}\left(2\theta K_0(\theta) + K_1(\theta)\right) - 2\left(e^{2\theta}+1\right)\right],$$
$$d_4 = \frac{2}{\Delta}\lambda e^{\theta}\left(I_1(\theta) - 2\theta I_0(\theta)\right), \qquad (21)$$
$$\Delta = \left((2\theta+1)\left(e^{2\theta}+1\right) - 2\right) I_1(\theta) -$$
$$-\left((2\theta+3)\left(e^{2\theta}-1\right)+6\right) I_0(\theta) - \left(2\theta^2 - \frac{3}{2}\right)e^{\theta}.$$

From the equation $w(r,0) = \frac{\partial F}{\partial t}$ we obtain the dependence of the amplitude on time in the same form as before (18). In this case the function f has the following form

$$f(\theta) = \frac{3\left(\frac{\theta}{2} - \cosh(\theta) I_1(\theta)\right)}{\left(2\theta I_1(\theta) - 3I_0(\theta)\right)\cosh(\theta) + \left(I_1(\theta) - 2\theta I_0(\theta)\right)\sinh(\theta) - \theta^2 + \frac{3}{4}}. \qquad (22)$$

ISSN 1814-4225 (print)
ISSN 2663-2012 (online)

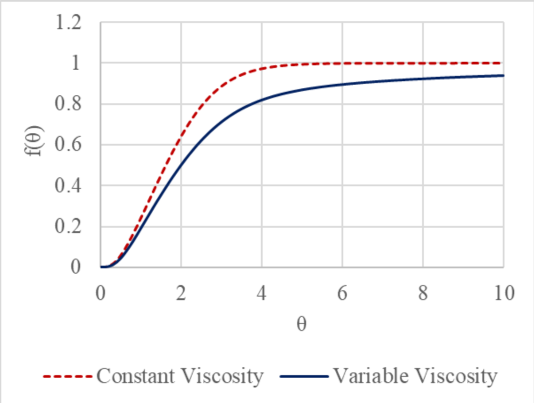

Fig. 9. Functions at constant and variable viscosities f(θ)

The difference between this function and a similar one obtained at constant viscosity (16) is shown in Fig. 9. This function has the same qualitative character, but leads to lower smoothing rates, which is explained by the higher average viscosity. It is clear that if we are talking about smoothing a periodic elongated inequality (Fig. 1,*a*) with variable viscosity, then we will have the same solution (20)–(22) with the difference that $\theta_n = \lambda_n h = n\pi \frac{h}{l}$, and not $\theta_n = \lambda_n h = b_n \frac{h}{R}$, as in this case.

7. Arbitrary Free Surface Shape

The presented analytical solutions are suitable for modelling arbitrary free surface shapes. To do this, the surface shape must be expanded into a Fourier series in terms of the functions $J_0(\lambda_n r)$ on the segment $-R \le r \le R$ (13). Let us show this by the example of a step function $F = H\left(r + \frac{R}{3}\right) - H\left(r - \frac{R}{3}\right) - \frac{1}{9}$, where H is the Heaviside function, which defines a cylindrical projection. The first five terms in the Fourier series have the following form

$$F = 0.55446 J_0(\lambda_1 r) + 0.56202 J_0(\lambda_2 r) + \\ +0.19223 J_0(\lambda_3 r) - 0.22537 J_0(\lambda_4 r) - \\ -0.35860 J_0(\lambda_5 r) + \ldots$$

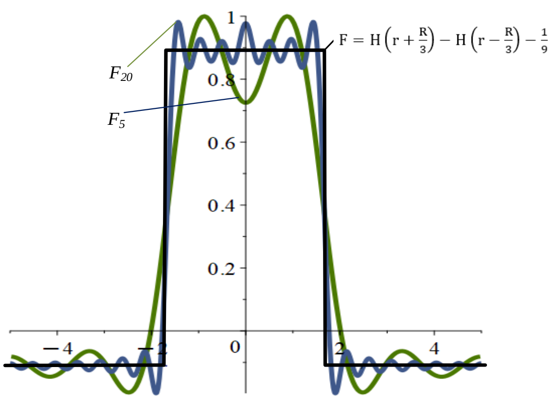

Fig. 10. Approximation of a step function by a Fourier series using Bessel functions

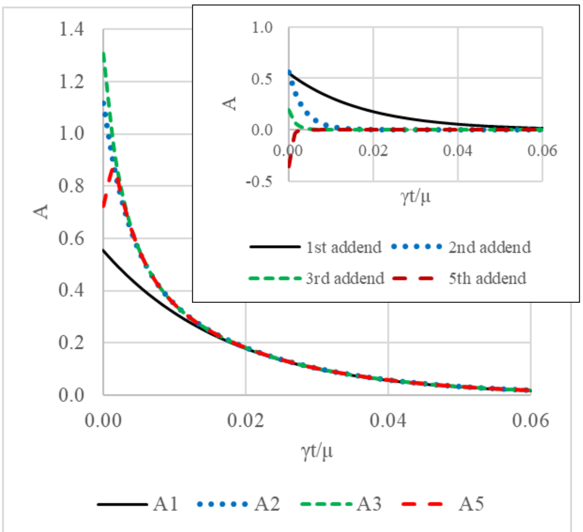

Fig. 11. Refinement of the solution by increasing the series terms from one (A1) to five (A5) and changing the in time of individual terms

The presence of corner points in the function being approximated (poor smoothness) leads to slow convergence of the Fourier series (Fig. 10). In addition, there is a significant gradient of the free surface; therefore, in this example, regardless of the accuracy of the analytical solution, we show only that to determine the surface smoothing time, it is sufficient to keep only the first term in the Fourier series.

The change in amplitude at the center ($r = 0$) as a function of time, for example, when $h = R = 1$ mm is written as

$$A(t) = 0.55446\, e^{-56.222\frac{\gamma t}{\mu}} + 0.56202\, e^{-288.08\frac{\gamma t}{\mu}} + \\ +0.19223\, e^{-664.59\frac{\gamma t}{\mu}} - 0.22537\, e^{-1101.2\frac{\gamma t}{\mu}} - \\ -0.35860\, e^{-1522.0\frac{\gamma t}{\mu}} + \ldots$$

The disadvantage of such a solution is that it complicates the determination of the time required for smoothing the surface, but if we consider the arguments of the exponential functions, we see that they grow rapidly, that is, the contribution of the second and subsequent functions is significant at the initial time point (at small t), over time these terms quickly decay and become undesirably small compared to the first term.

Therefore, if we are interested in the time during which the amplitude decreases almost to zero, then it is enough to consider only one first term; the other terms refine the solution only at the initial stages. This situation is illustrated in Fig. 11.

8. Discussion

The scientific novelty of this study lies in the fact that it further develops Orchard's formula by extending it to axisymmetric problems (18). The obtained analytical solution correlates well with the numerical solution for moderate and thick layers ($h > 0.2R$). The use of the obtained analytical solutions is limited to the initial height of the surface amplitude (up to 40% of the radius). It remains valid under the assumptions described in Section 2. An analytical solution to the problem of variable viscosity over the thickness of the liquid layer (formulas (18)+(22)) is obtained. The solution covers both periodic and axisymmetric problems.

The obtained simple analytical solutions allow us to solve the main task – determining the surface smoothing time. The time required to reduce the height of the bulge (unevenness, roughness) by a factor of $k = \frac{A_0}{A(t)} > 1$ calculated using the following formula

$$t = \ln(k) \frac{2\mu}{\gamma\lambda f(\theta)}.$$

In this formula μ is the dynamic viscosity; γ is the surface tension; the function $f(\theta)$ is determined by formula (16) for the same viscosity of the entire liquid and by formula (22) if the viscosity changes from a finite value on the free surface (μ) to infinity on the solid surface; $\theta = \lambda h$; h is the average height; $\lambda = \frac{\pi}{l}$ if we are talking about a periodic problem (Fig. 1,*a*) and $\lambda = \frac{b_1}{R} = \frac{3.8317060}{R}$ in the axisymmetric case (Fig. 1,*b*). To estimate the levelling time of a surface whose shape is different from the shape of the Bessel function J_0 in an axisymmetric problem (Fig. 1,*b*) or cos in a periodic problem (Fig. 1,*a*), it is sufficient to use the first function in the expansion of the free surface shape function into a Fourier series (point 6).

9. Conclusions

The main contribution of this research is that the obtained analytical solutions provide a comprehensive framework for predicting the surface levelling dynamics of viscous liquids under surface tension forces, with a particular focus on the thermal energy treatment of plastic surfaces. Solving the research tasks, in particular the extension of Orchard's formula to axisymmetric surface irregularities and taking into account viscosity variations in the liquid layer, improved the understanding of surface smoothing mechanisms in complex geometries, thereby achieving the research goal, namely, filling the gap in existing analytical leveling models. The derived analytical model, validated against numerical simulations, demonstrated high accuracy for moderate-to-thick liquid layers ($h > 0.2R$) and initial surface amplitudes up to 40% of the characteristic radius, making it a reliable tool for process optimization.

The results demonstrate the model's ability to predict levelling times efficiently while maintaining simplicity. The addition of thickness-dependent viscosity further improves its applicability to real-world scenarios in which material properties vary with temperature. These findings offer practical benefits for industrial applications, particularly for optimizing heat input and process parameters to improve surface quality. By providing explicit expressions for levelling time, the model enables precise control over surface evolution, thereby reducing trial-and-error in thermal treatment processes.

While this study primarily focused on theoretical and numerical validation, future work will explore experimental validation to further assess the model's accuracy under practical conditions. Further refinements will enhance the predictive capabilities by incorporating more complex material behaviors, such as non-Newtonian effects or transient thermal gradients. The integration of this analytical approach with advanced manufacturing techniques could lead to improved surface engineering strategies, contributing to the development of more efficient and controlled thermal treatment processes in industrial applications.

Contributions of authors: conceptualization, methodology – **Vitalii Myntiuk**, **Olga Shypul**; formulation of tasks, analysis – **Vitalii Myntiuk**, **Oleh Tryfonov**; development of models, verification – **Vitalii Myntiuk**, **Oleh Tryfonov**; analysis of results, visualization – **Vitalii Myntiuk, Olga Shypul, Yevgen Tsegelnyk**; writing – original draft preparation – **Vitalii Myntiuk**, **Olga Shypul**; writing – review and editing – **Olga Shypul**, **Yevgen Tsegelnyk.**

Conflict of Interest

The authors declare that they have no conflict of interest concerning this research, whether financial, personal, authorship or otherwise, that could affect the research, and its results presented in this paper.

Financing

This study received funding from the EURIZON project, which is funded by the European Union (Grant Agreement No.871072).

Data Availability

The data associated with this work are stored in the data repository.

Use of Artificial Intelligence

The authors confirm that they did not use artificial intelligence methods in their work.

Acknowledgments

This study was supported by the European Union Assistance Instrument for the Fulfilment of Ukraine's Commitments under the Horizon 2020 Framework Program for Research and Innovation (Research Project No. 0124U004371).

All authors have read and agreed to the published version of the manuscript.

References

1. Kurdi, A., & Chang, L. Recent advances in high performance polymers – tribological aspects. *Lubricants*, 2018, vol. 7, iss. 1, article no. 2. DOI: 10.3390/lubricants 7010002.
2. Pedroso, A. F., Sebbe, N. P., Silva, F. J., Campilho, R. D., Sales-Contini, R. C., Costa, R. D., ... & Nogueira, F. R. A concise review on materials for injection moulds and their conventional and non-conventional machining processes. *Machines*, 2024, vol. 12, iss. 4, article no. 255. DOI: 10.3390/machines12040255.
3. Vambol, O., Kondratiev, A., Purhina, S., & Shevtsova, M. Determining the parameters for a 3D-printing process using the fused deposition modeling in order to manufacture an article with the required structural parameters. *Eastern-European Journal of Enterprise Technologies*, 2021, vol. 2, no. 1, pp. 70–80. DOI: 10.15587/1729-4061.2021.227075.
4. Wickramasinghe, S., Do, T., & Tran, P. FDM-based 3D printing of polymer and associated composite: A review on mechanical properties, defects and treatments. *Polymers*, 2020, vol. 12, iss. 7, article no. 1529. DOI: 10.3390/polym12071529.
5. Plankovskyy, S., Popov, V., Shypul, O., Tsegelnyk, Y., Tryfonov, O., & Brega, D. *Advanced thermal energy method for finishing precision parts*. In Advanced Machining and Finishing; Gupta, K., Pramanik, A., Eds.; Elsevier: Amsterdam, Netherlands, 2021, pp. 527–575. DOI: 10.1016/B978-0-12-817452-4.00014-2.
6. Adel, M., Abdelaal, O., Gad, A., Nasr, A. B., & Khalil, A. Polishing of fused deposition modeling products by hot air jet: evaluation of surface roughness. *Journal of Materials Processing Technology*, 2018, vol. 251, pp. 73–82. DOI: 10.1016/j.jmatprotec.2017.07.019.
7. Chai, Y., Li, R. W., Perriman, D. M., Chen, S., Qin, Q. H., & Smith, P. N. Laser polishing of thermoplastics fabricated using fused deposition modelling. *The International Journal of Advanced Manufacturing Technology*, 2018, vol. 96, no. 9, pp. 4295–4302. DOI: 10.1007/s00170-018-1901-5.
8. Plankovskyy, S., Shypul, O., Tsegelnyk, Y., Brega, D., Tryfonov, O., & Malashenko, V. *Basic principles for thermoplastic parts finishing with impulse thermal energy method*. In Handbook of Research on Advancements in the Processing, Characterization, and Application of Lightweight Materials; Kumar, K., Babu, B., Davim, J., Eds. IGI Global: Hershey PA, USA, 2022, pp. 49–87. DOI: 10.4018/978-1-7998-7864-3.ch003.
9. Orchard, S. E. On surface levelling in viscous liquids and gels. *Applied Scientific Research, Section A*, 1963, vol. 11, pp. 451–464. DOI: 10.1007/BF03184629.
10. Wapler, D. Das rheologische Verhalten der Anstrichstoffe bei der Verarbeitung (2a) – Untersuchungen über das Verlaufen. *Farbe und Lack*, 1975, vol. 81, no. 8, pp. 717–723.
11. Overdiep, W. S. The levelling of paints. *Progress in Organic Coatings*, 1986, vol. 14, iss. 2, pp. 159–175. DOI: 10.1016/0033-0655(86)80010-3.
12. Weidner, D. E. Leveling of a model paint film with a yield stress. *Journal of Coatings Technology and Research*, 2020, vol. 17, no. 4, pp. 851–863. DOI: 10.1007/s11998-019-00260-z.
13. Seeler, F., Hager, C., Tiedje, O., & Schneider, M. Simulations and experimental investigation of paint film leveling. *Journal of Coatings Technology and Research*, 2017, vol. 14, no. 4, pp. 767–781. DOI: 10.1007/s11998-017-9934-5
14. Klarskov, M., Jakobsen, J., & Saarnak, A. Verification of the Orchard leveling analysis. *Rheology*, 1992, vol. 92, pp. 30–39.
15. Xie, Y., Zhao, T., & Liu, K. Theoretical modeling of key parameters of wet film in roll coating process of coating panel. *AIP Advances*, 2023, vol. 13, no. 12, article no. 125224. DOI: 10.1063/5.0185600.
16. Schiltz, A. Analysis of surface tension in terms of force gradient per unit area. *arXiv Preprint*, 2024, arXiv no. 2406.16448. DOI: 10.48550/arXiv.2406.16448.
17. Takahashi, Y., Tanaka, G., Chang, F., Kato, F., & Iwata, H. Numerical analysis of sagging based on rheological properties of a paint film and proposal for a novel index to evaluate the amount of sag. *IEEE Transactions on Automation Science and Engineering*, 2023, vol. 21, iss. 3, pp. 2237–2250. DOI: 10.1109/ TASE.2023.3337280.
18. Smetankina, N. V., Postnyi, O. V., Merkulova, A. I., & Merkulov, D. O. Modeling of non-stationary temperature fields in multilayer shells with film heat sources. *2020 IEEE KhPI Week on Advanced Technology (KhPIWeek)*, Kharkiv, Ukraine, IEEE, 2020, pp. 242–246. DOI: 10.1109/KhPIWeek51551.2020.9250139.
19. Shypul, O., & Myntiuk, V. Transient thermoelastic analysis of a cylinder having a varied coefficient of thermal expansion. *Periodica Polytechnica Mechanical Engineering*, 2020, vol. 64, no. 4, pp. 273–278. DOI: 10.3311/PPme.14733.
20. Boschetto, A., Bottini, L., & Veniali, F. Finishing of fused deposition modeling parts by CNC machining. *Robotics and Computer-Integrated Manufacturing*, 2016, vol. 41, pp. 92–101. DOI: 10.1016/j.rcim.2016.03.004.
21. Jin, Y., Wan, Y., Zhang, B., & Liu, Z. Modeling of the chemical finishing process for polylactic acid parts in fused deposition modeling and investigation of its tensile properties. *Journal of Materials Processing Technology*, 2017, vol. 240, pp. 233–239. DOI: 10.1016/ j.jmatprotec.2016.10.003.
22. Fritz, A., Sekol, L., Koroskenyi, J., Walch, B., Minear, J., Fernandez, V., & Liu, L. Experimental analysis of thermal energy deburring process by design

of experiment. *Proceedings of the ASME 2012 International Mechanical Engineering Congress and Exposition*, ASME, 2012, vol. 3, pp. 2035–2041. DOI: 10.1115/IMECE2012-88411.

23. Pan, X., Wu, C. T., & Hu, W. Incompressible Smoothed Particle Galerkin (ISPG) method for an efficient simulation of surface tension and wall adhesion effects in the 3D reflow soldering process. *16th International LS-DYNA Users Conference*, ANSYS, 2020, pp. 1–17.

24. Zhang, X., Cao, C., Gui, N., Huang, X., Yang, X., Tu, J., Jiang, S., & Zhao, Q. A particle-scale model of surface tension for two-phase flow: model description and validation. *Energies*, 2022, vol. 15, iss. 19, article no. 7132. DOI: 10.3390/en15197132.

Received 17.10.2024, Accepted 17.02.2025

ОСЕСИМЕТРИЧНА ЗАДАЧА ЗГЛАДЖУВАННЯ ПОВЕРХНІ В'ЯЗКОЇ РІДИНИ ПІД ДІЄЮ СИЛ ПОВЕРХНЕВОГО НАТЯГУ

В. Б. Минтюк, О. В. Шипуль, О. В. Трифонов, Є. В. Цегельник

У цьому дослідженні розглядається аналітичне розв'язання задачі вирівнювання поверхні в'язких рідин під впливом сил поверхневого натягу, зосереджуючись на згладжуванні пластикових поверхонь під час їхнього термоенергетичного оброблення. **Метою** роботи є розширення формули Орчарда на осесиметричні нерівності поверхні та розроблення аналітичної моделі для прогнозування часу вирівнювання, що забезпечить ефективний контроль процесу термоенергетичного оброблення. **Завдання** дослідження включали виведення аналітичного розв'язку для осесиметричного вирівнювання, його верифікацію за допомогою числових моделювань у LS-DYNA та врахування зміни в'язкості в межах рідинного шару. **Методи** дослідження передбачали аналітичну формалізацію та числове моделювання еволюції поверхні, з урахуванням різних початкових геометрій нерівностей та розподілу в'язкості. Верифікація аналітичного рішення на основі числових розрахунків показала високу точність для середніх і товстих рідинних шарів ($h > 0.2R$) та початкових амплітуд нерівностей до 40% від характеристичного радіуса. Після верифікації модель була застосована для оцінки часу вирівнювання різних конфігурацій поверхні, зберігаючи простоту при підвищенні прогностичної точності. **Результати** показали, що розширена формула ефективно описує динаміку згладжування поверхні, включаючи випадки з в'язкістю, що змінюється залежно від товщини шару, та забезпечує явні вирази для розрахунку часу вирівнювання. Отримані результати дозволяють точно контролювати теплове навантаження під час термічного оброблення, оптимізуючи якість поверхні. **Висновки**. Запропоновані аналітичні рішення є практичним інструментом для аналізу вирівнювання поверхонь, розширюючи застосування підходу Орчарда на більш складні геометрії та варіації в'язкості. Подальші дослідження будуть зосереджені на експериментальній перевірці та подальшому вдосконаленні моделей для підвищення точності у промислових застосуваннях.

Ключові слова: згладжування поверхні; формула Орчарда; осесиметричні нерівності; постановка періодичної задачі.

Минтюк Віталій Борисович – канд. техн. наук, доц. каф. проєктування літальних апаратів, Національний аерокосмічний університет «Харківський авіаційний інститут», Харків, Україна.

Шипуль Ольга Володимирівна – д-р техн. наук, доц., проф. каф. технології виробництва літальних апаратів, Національний аерокосмічний університет «Харківський авіаційний інститут», Харків, Україна.

Трифонов Олег Валерійович – канд. техн. наук, доц., доц. каф. технології виробництва літальних апаратів, Національний аерокосмічний університет «Харківський авіаційний інститут», Харків, Україна.

Цегельник Євген Володимирович – канд. техн. наук, старш. досл., заст. директора з наукової роботи навчально-наукового інституту енергетичної, інформаційної та транспортної інфраструктури, Харківський національний університет міського господарства ім. О. М. Бекетова, Харків, Україна.

Vitalii Myntiuk – Candidate of Technical Sciences, Associate Professor at the Department of Aircraft Design, National Aerospace University "Kharkiv Aviation Institute", Kharkiv, Ukraine,
e-mail: vitalii.myntiuk@khai.edu, ORCID: 0000-0002-4047-0192, Scopus Author ID: 57201067344.

Olga Shypul – Doctor of Technical Sciences, Associate Professor, Professor at the Department of the Technologies of Aircraft Manufacturing, National Aerospace University "Kharkiv Aviation Institute", Kharkiv, Ukraine, e-mail: o.shipul@khai.edu, ORCID: 0000-0002-1356-5831, Scopus Author ID: 57192959380.

Oleh Tryfonov – Candidate of Technical Sciences, Associate Professor, Associate Professor at the Department of the Technologies of Aircraft Manufacturing, National Aerospace University "Kharkiv Aviation Institute", Kharkiv, Ukraine, e-mail: o.v.trifonov@gmail.com, ORCID: 0000-0001-8058-8649, Scopus Author ID: 57192959255.

Yevgen Tsegelnyk – Candidate of Technical Sciences, Senior Researcher, Deputy Head (Research) at the School of Energy, Information and Transport Infrastructure, O.M. Beketov National University of Urban Economy in Kharkiv, Kharkiv, Ukraine, e-mail: y.tsegeknyk@kname.edu.ua, ORCID: 0000-0003-1261-9890, Scopus Author ID: 57192961558.